

# Dynamic Modelling and Implementation of VSC-HVDC System

## The Grid Connected Large Offshore Wind Power Plant Application

Muhammad Raza\* and Oriol Gomis-Bellmunt†

Centre d'Innovació Tecnològica en Convertidors Estàtics i Accionaments, Departament d'Enginyeria Elèctrica,  
Universitat Politècnica de Catalunya, 08028 Barcelona, Spain

**Keywords:** VSC-HVDC, Power System Analysis, Wind Farm Integration, DC Transmission System, Power System Modelling.

**Abstract:** This research contribution, investigates and analyse the operational characteristics of a voltage source converter (VSC), High-Voltage Direct Current (HVDC) transmission system. The main objective of this research endeavor is to evaluate the implementation of a HVDC transmission system for integrating offshore wind energy with the grid. Dynamic model of the system is developed in the Simulink environment. Stability analysis has been performed through three case studies namely the two active grid interconnection, active and passive grid interconnection and the offshore wind farm interconnection with the grid. Results are analysed and compared according to E.ON grid code requirements for offshore grid connection.

## NOMENCLATURE

$i, u$	complex current, voltages
$p, q$	active power, reactive power
$l, c, r$	inductance, capacitance, resistance
$P_m$	modulation index
$K, T$	gain constant, time constant
$\omega$	angular speed
<b>Subscripts</b>	
$r, i$	real, imaginary component
$d, q$	direct, quadrature axis component

Sign Convention: load oriented; consumed active and inductive reactive power are considered positive.

## 1 INTRODUCTION

Wind energy is one of the leading and foremost sources of energy in reducing the greenhouse-gas emission. According to the European Wind Energy Association, 9,616MW of wind energy was installed

in the European Union during 2011, among which 8,750MW was onshore and 866MW offshore(Wilkes, 2010).

According to wind distribution theory, roughness class at sea level is lower than at ground. Lower roughness class means less obstacles and low wind speed variation. This predict that wind farm at offshore could have higher capacity as compare to onshore site. For short distance offshore site from land, HVAC transmission system is suitable as, it is least expensive, evolve and conventional technology for grid integration. However, at longer transmission distance due to cable capacitance, reactive losses increases significantly. Typically, HVAC transmission length is limited to 120km for offshore connection. HVDC system has some advantages over HVAC but it has higher development cost(Hulle and Gardner, 2010).

Nowadays, transmission and distribution system operators are giving significant consideration to HVDC transmission system. Past researches has established an idea that in comparison to HVAC for longer distance, HVDC transmission system is a suitable solution for transferring a large amount of energy, but beside that it is also very important to ensure that HVDC system should fulfills the grid compliances and perform similar as conventional transmission system.

General grid code defines the operational limits

\*The research leading to these results has received funding from the People Programme (Marie Curie Actions) of the European Unions Seventh Framework Programme (FP7/2007-2013) under REA grant agreement n 317221.

†The project is also supported by the Ministerio de Economía y Competitividad, Plan Nacional de I+D+i under Project ENE2012-33043.

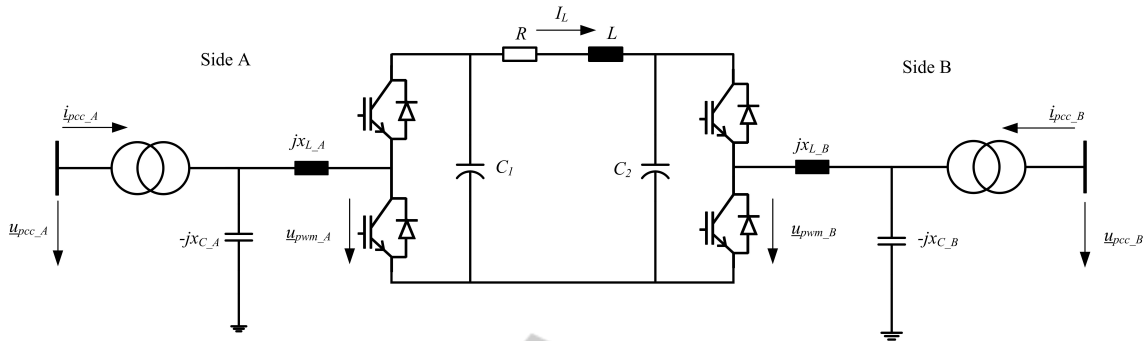


Figure 1: Point-to-Point Voltage-Source-Converter High Voltage Direct Current Transmission System Configuration.

and characteristic that a system must exhibit at point of common coupling (PCC). These limits are defined in terms of voltage levels, frequency deviation and duration limits, reactive power capability, fault condition, and active power control. The E.ON grid code compliances for offshore wind farm integration with the grid summarized as follows (E.ON, 2008) (E.ON, 2006).

1. **Voltage Stability:** The nominal voltage ( $U_n$ ) level of the grid is 155kV and continuous operational voltage range is 140-170kV. Wind generators should not be disconnected if voltage decreases  $0.8U_n$  up to 3s, and voltage increase  $1.2U_n$  up to 200ms.
2. **Active Power Control and Frequency Limits:** If frequency at PCC bus drops to 46.5Hz or rises above 53.5Hz then all wind turbines must be disconnected within 300ms. If grid frequency is in the range of 46.5-47.5Hz or 51.5-53.5Hz then turbines are only allowed to disconnect after 10s. After fault recovery in order to stabilize the voltage level, increase in active power per minute is permissible at maximum rate of 10% of  $P_n$ . If grid frequency exists within the range of 50.1Hz to 51.5Hz, active power must decrease at the rate of 98% per Hz and 25% per second.
3. **Reactive Power Control:** Within the voltage range of  $\pm 0.05U_n$ , and at power generation from maximum to  $0.2P_n$ , wind turbines must be capable of supplying reactive power up to  $0.4P_n$  in over-excited and  $-0.3P_n$  in under-excited condition. At PCC bus power factor must be controlled within the range of 0.925 lagging to 0.95 leading.
4. **Fault-Ride-Through Capability:** During fault, wind turbines must inject additional reactive current into PCC bus in order to support the voltage level. Voltage support must be provided when voltage drop is equal to or greater than 5% of generator rated voltages. Voltage support control system should

be activated within 20ms after fault detection. The amount of additional reactive power injection depends on nominal voltage and rated current of the wind generator. Wind turbine must not be disconnected if voltage drops to  $0.15U_n$  for 600ms.

Although, Voltage Source Converter (VSC) transmission system is new as compared to Line Commutator Converter (LCC) but it provides some advantages such as, option to control the active and reactive power flow independently, low harmonics, black or passive start, low or no reactive power requirement at no-load and bi-directional power flow.

In VSC, principle of a converter control system is based on (1). Power flow between converter and network is controlled by varying voltage magnitude and phase angle.

$$P = \frac{U_{pcc} U_{pwm} \sin \delta}{\omega l} \quad (1)$$

$$Q = \frac{1}{\omega l} \{ U_{pwm}^2 - U_{pcc} U_{pwm} \cos \delta \}$$

## 2 VSC-HVDC SYSTEM MODELLING

The architecture of the VSC-HVDC transmission system developed is shown in Fig. 1. In this configuration, two points (defined as PCC bus) are connected via two VSC systems and DC cables. PCC bus could be a connection point of a grid, island network (passive load), or wind farm. Bi-directional power among these two buses flows according to VSC control mode.

System is divided into three sections for modelling; VSC (converter/inverter), DC transmission line, and AC network. PWM-Converter is connected with the grid through coupling reactance. Coupling reactance stabilizes the AC current, reduces the fault current, helps to reduce the harmonic current content

and enables the control of power flows from the voltage source converter. Typically, AC filter and converter reactor transform the non-sinusoidal output of converter into sinusoidal output.

The transformer is an ordinary single phase or three-phase power transformer, with a tap changer. The secondary voltage (filter bus) is control with the tap changer to achieve the maximum active and reactive power from the converter (both consumption and generation). In order to maximize the power transfer, low frequency zero-sequence voltage generated by the converter, is block by un-grounding the transformer secondary winding(Wang et al., 2009). Moreover, ability of VSC system to support the grid stability depends on three factors:

- **Rated Current of IGBTs:** According to (3), DC power is equal to AC active power. Since, maximum current flow is limited by IGBTs, therefore at rate power, MVA capability decreases if AC voltage drops.
- **DC Voltage Level:** Maximum AC voltage generated by VSC depends upon maximum DC voltage. Also, the amount of reactive power flow is proportional to the voltage difference of PCC and converter bus voltage. The reactive power capability of a converter is low if the difference between DC level and grid voltage is low.
- **Rated DC Current:** Maximum active power flow depends on the current carrying capacity of DC cable.

## 2.1 Voltage Source Converter (VSC) Model

In Simulink for RMS simulation, converter is model using DC voltage controlled AC voltage source and output signal is depend on modulation index. Complex AC voltage generated by the converter is calculated using (2). For simplicity, it is assume that there are no losses in the converter thus, power balancing equation is completed using (3). Converter can act as rectifier or inverter depending upon operation mode and set-points.

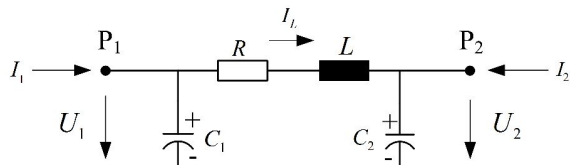


Figure 2: Equivalent Model of DC Cable.

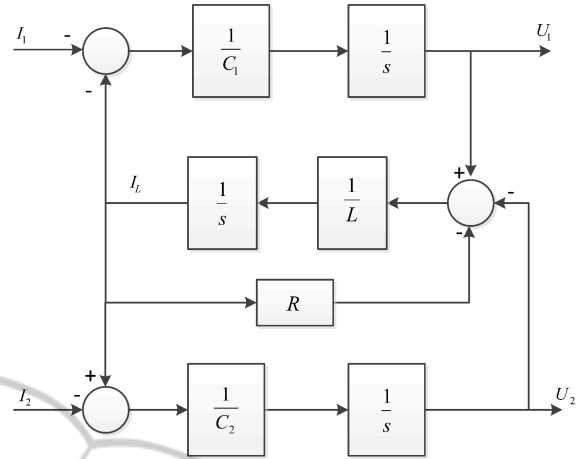


Figure 3: Simulink Control Diagram of DC Cable.

$$\begin{aligned} U_r &= K_0 P_{mr} U_{dc} \\ U_i &= K_0 P_{mi} U_{dc} \end{aligned} \quad (2)$$

$$P_{ac} = \Re(\underline{u}_{ac} \cdot \underline{i}_{ac}^*) = U_{dc} I_{dc} = P_{dc} \quad (3)$$

## 2.2 DC Transmission Line

DC cable is modelled as a  $\pi$ -link as shown in Fig. 2. Cable capacitance is divided into two parts and added with capacitance of the converter capacitance. In DC transmission only active power flows, therefore, line inductance is small enough to neglect, but it is included in model to complete the differential equation(Bao et al., 2011). Control system diagram of the transmission system is shown in Fig. 3.

## 2.3 AC Network System

AC network is consist of transformer, capacitor bank and series reactance. The system is represented as LCL network (inductance-capacitance-inductance). Characteristically, this configuration act as low pass T-filer as shown in Fig. 4. Transformer impedance and voltages are referred to the filter bus side. Using (4) and (5), we can represent AC system in  $dq0$ -coordinate system.

$$\begin{aligned} u_{pwm,d}^{\angle u_{pcc}} &= u_{pcc,d}^{\angle u_{pcc}} + \omega l_T i_{pcc,q}^{\angle u_{pcc}} + \omega l_L \left( i_{pcc,q}^{\angle u_{pcc}} \right. \\ &\quad \left. - \omega c u_{pcc,d}^{\angle u_{pcc}} \right) \end{aligned} \quad (4)$$

$$\begin{aligned} u_{pwm,q}^{\angle u_{pcc}} &= u_{pcc,q}^{\angle u_{pcc}} - \omega l_T i_{pcc,d}^{\angle u_{pcc}} - \omega l_L \left( i_{pcc,d}^{\angle u_{pcc}} \right. \\ &\quad \left. + \omega c u_{pcc,q}^{\angle u_{pcc}} \right) \end{aligned} \quad (5)$$

### 3 HVDC CONVERTER CONTROL SYSTEM

Control system has five operational modes i.e. passive network control, active power control ( $P$ ), reactive power control ( $Q$ ), DC voltage control ( $U_{dc}$ ), and AC voltage control ( $U_{ac}$ ). The flow diagram of HVDC control system is shown in Fig. 5. Control modes are defined according to the operational requirement (Yuan and Wang, 2012).

1.  $U_{dc} - Q$ : In this mode, DC-voltage and reactive power set-points are given. Usually, this mode is defined at the grid side converter to integrate passive load with active grid.
2.  $U_{ac} - P$ : In this mode, AC-voltage magnitude and active power set-points are given. This mode is set to integrate two active grids.
3.  $P - Q$ : This mode specifies active and reactive power set-points. Through, this mode  $PQ$  characteristic of a system is determined.
4.  $U_{ac} - U_{dc}$ : This mode specifies AC and DC voltage set-points.
5. *Passive Network Control*: In this mode, converter operates as a slack node (magnitude and phase control). Set at passive network or wind farm side converter control.

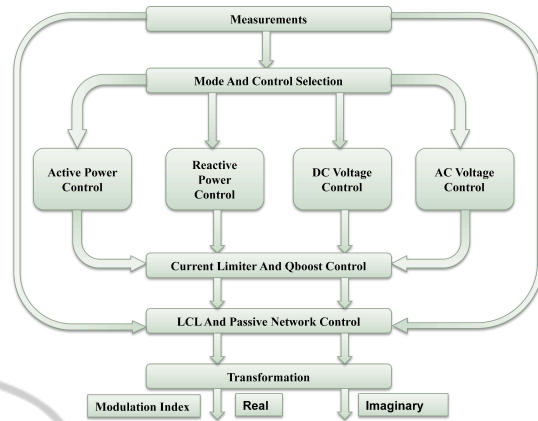


Figure 5: Voltage Source Converter Control Architecture.

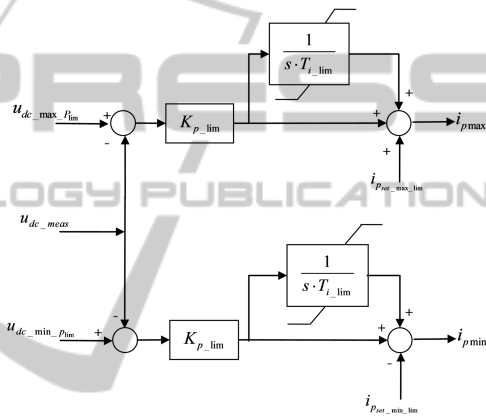


Figure 6: Dynamic Limits for Active Power Control.

#### 3.1 Active Power Control

In this mode, active power flow is control at PCC bus at desire value. An adaptive closed-loop proportional-plus-integral control system is developed for active power control. In voltage oriented reference system, for the condition  $u_{pcc,d} = 1.0p.u$ , the active current reference can be obtained using control configuration shown in Fig. 7. Active power flow from AC to DC network raises the DC voltage. If there is large imbalance in power at both side then DC voltage will

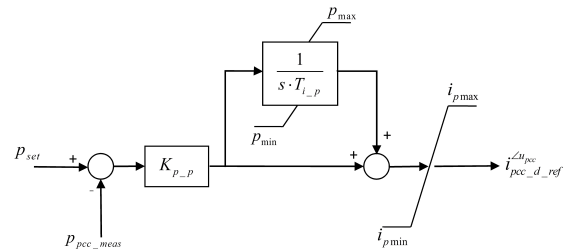


Figure 7: Proportional Plus Integral Controller for Active Power Control.

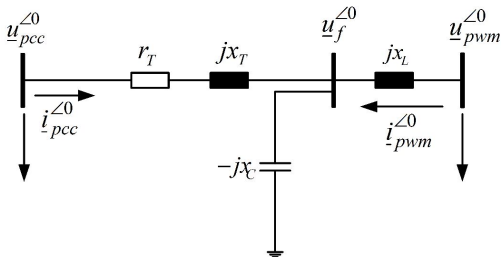


Figure 4: Phasor Representation of Transformer Impedance, Series Reactance and Filter Capacitor as LCL Network.

exceed the maximum operating voltage limit of cable. Furthermore, when transferring large power over a long distance, DC voltage difference between sending end and receiving end will be high due to line resistive losses.

Therefore, it is needed to limit the power flow according to maximum permissible DC voltage. Dynamic saturation limits shown in Fig. 6, are applied at the output of proportional-plus-integral controller.

### 3.2 Reactive Power Control

In this mode, reactive power flow is control at PCC bus at desire value. In voltage oriented reference system, reactive power can be controlled by reactive current reference using (6). PI control configuration is calculated using (7).

$$q_{set} = i_m \sin \delta = -i_{pcc-q.ref}^{\angle u_{pcc}} \quad (6)$$

Reactive power demand depends on the PCC bus voltage. Often, it is defined in grid code to have a power factor within the range of 0.925 overexcited and 0.95 in under-excited operation. Thus, according to  $PQ$  characteristic maximum permissible reactive power flow is approx. 55% of rated power.

$$i_{pcc-q.ref}^{\angle u_{pcc}} = \left\{ K_{p-q} \left( 1 + \frac{1}{s \cdot T_{i-q}} \right) \right\} \cdot (-q_{set} + q_{meas}) \quad (7)$$

### 3.3 DC Voltage Control

In this mode, converter control the DC voltage at desire value. Active AC and DC power transmitted over a DC cable using voltage source converter is calculated using (8) and (9).

$$P_{ac} = U_d I_d + U_q I_q \quad (8)$$

$$P_{dc} = U_{dc} I_{dc} \quad (9)$$

In balance rotating, synchronous frame in voltage oriented system,  $dq0$  voltages are constant. Such that  $U_q$  and  $U_0$  are zero and  $U_d$  is rated voltage. Imbalance in AC and DC power leads to a change in DC voltage level across DC capacitors. Voltage across the capacitors is calculated using (10).

$$C \frac{\partial U_{dc}}{\partial t} = \frac{1}{U_{dc}} \{ P_{ac} - P_{dc} \} \quad (10)$$

To maintain the constant DC level at rated voltage, system must fulfill condition (11).

$$\begin{aligned} P_{ac} &= P_{dc} \\ U_d I_d &= U_{dc} I_{dc} \end{aligned} \quad (11)$$

From (11), it is obvious that DC voltage can be controlled through the  $d$ -component of reference current. The PI control system implementation for DC voltage control is shown in Fig. 8. Maximum and minimum permissible voltage levels are 120% and 90% of rated DC cable voltage, respectively.

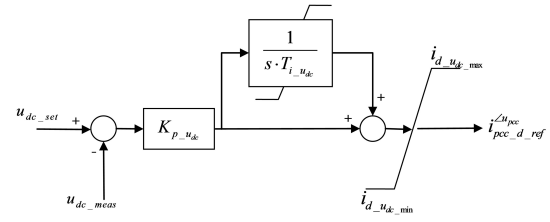


Figure 8: Proportional Plus Integral Control for DC Voltage Control.

### 3.4 AC Voltage Control

In this mode, AC voltage of PCC bus is control at desire value. It is obvious from (1) that reactive power flow can be control by controlling voltage difference between converter and PCC bus. Thus, voltage drop across transformer and line reactance together can be calculated using (12). In  $dq0$  balance voltage oriented synchronous frame, reactive power is controlled by  $q$ -component of the reference current, consequently controlling AC voltage level.

Close loop PI control system is implemented to control the AC voltage. In addition to that, washout filter is also incorporated to block the high frequency noise in input signals. The control diagram of AC voltage control is shown in Fig. 9.

$$\begin{aligned} \Delta u &= u_{pcc}^{\angle 0} - u_{pwm}^{\angle 0} \\ &\approx (r \cdot i_d - x \cdot i_q) + j(x \cdot i_d + r \cdot i_q) \quad (12) \\ &\approx -x \cdot i_{q.ref}^{\angle u_{pcc}} + jx \cdot i_{d.ref}^{\angle u_{pcc}} \end{aligned}$$

### 3.5 Passive Network Control

Passive network control is designed for operating wind farm and consumer load. In this mode, PCC bus acts as an active node i.e. voltage magnitude of converter bus is adapted according to load impedance, such that voltage level at PCC bus controlled to 1.0p.u. Passive network control equations is derived using (13).

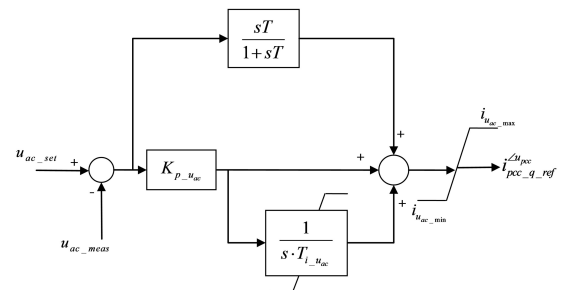


Figure 9: AC Voltage Control of Voltage Source Converter with Washout Filter.

$$\begin{aligned} u_{pwm.d}^{\angle u_{pcc}} &= u_{pcc.d}^{\angle u_{pcc}} + x_T \cdot i_{pcc.q}^{\angle u_{pcc}} + x_L \cdot i_{pwm.q}^{\angle u_{pcc}} \\ u_{pwm.q}^{\angle u_{pcc}} &= -x_T \cdot i_{pcc.d}^{\angle u_{pcc}} - x_L \cdot i_{pwm.d}^{\angle u_{pcc}} \end{aligned} \quad (13)$$

Voltage stability depends upon the demand of reactive power. The droop Characteristics for voltage set point is implemented to generate or absorb the reactive power. A droop characteristic for the voltage controller is demonstrated in Fig. 10. Since, reactive power flows from higher voltage level to lower voltage level, therefore, set-point of voltage should be increased, when the demand for the reactive power increase. Droop control system is useful for supplying power to inductive load or wind farm with DFIG(Zhang and Lennart, 2011).

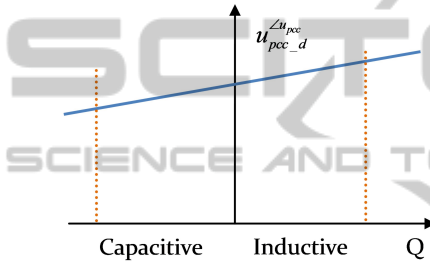


Figure 10: Droop Characteristic of Passive Network Control.

The voltage reference value is calculated using (14):

$$u_{pcc.d}^{\angle u_{pcc}} = u_{pcc.d.set}^{\angle u_{pcc}} + K \cdot q \quad (14)$$

## 4 DYNAMIC PERFORMANCE ANALYSIS

Dynamic response of HVDC system is evaluated using three case studies. Analysis are performed to evaluate the system ability to remain stable due to small disturbance during operation. Since, VSC-HVDC transmission will be used as an alternative of the convention AC transmission system, therefore, it is important to assess the performance of the system compatibility with the existing system. And, it is required to perform the operational capability tests such as, ability to transfer large power at long distance while maintaining voltage stability, independent active and reactive power control capability, ability to integrate weak grid, ability to supply power to island or passive network, and ability to integrate wind farm. For all case studies, approx. 100km transmission length is considered.

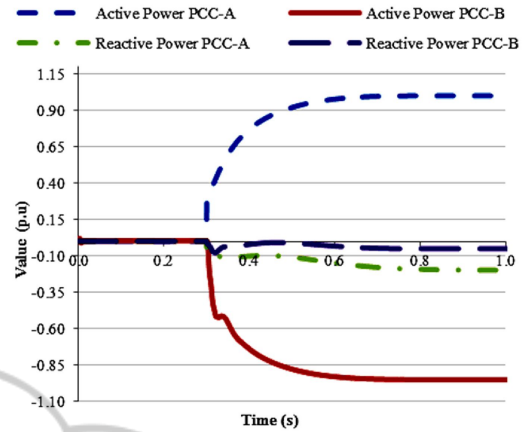


Figure 11: Power Flow Response of a HVDC System Interconnecting Two Active Grid.

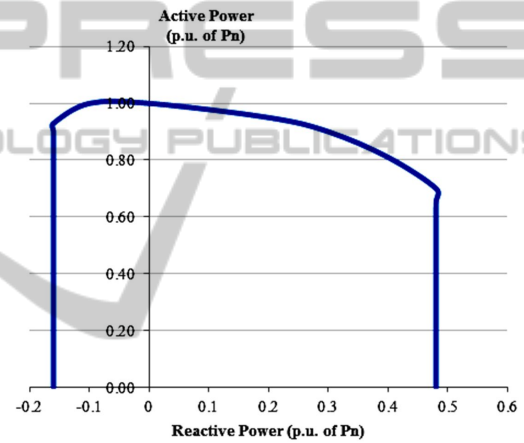


Figure 12: P-Q Diagram of 'Side-A' Converter with 100km Transmission Line.

### 4.1 Interconnection of Two Active Grids

In this study, transmission system describes in Fig. 1. is connected with two active grids each at both sides. Capacity of converter is approx. 200MW. 'Side-A' converter is set in  $P-Q$  mode and 'Side-B' converter is set in  $U_{dc}-Q$  mode. Initially,  $P-Q$  set-points are zero, therefore, no power flows. Step change in power demand from zero to full load at 0.3s is applied by changing  $P-Q$  set-points at 'Side-A' converter, which lead power to flow from side A to B. Due to sudden in-feed of active power into transmission system, DC voltage rises up to 1.16p.u. Increase in DC voltage level is proportional to the active power available to 'Side-B' converter to supply into network.

Power and voltage response of the network are shown in Fig. 11. and Fig. 13. respectively. It is to be notice that at set active power at 'Side-A', in order to stabilize the voltage level at PCC bus, 20% of  $P_n$  re-

active power injection is required. This is achieved by setting the reactive power set-point to  $-0.2p.u.$ . This demonstrates VSC control scheme capability to control active and reactive power independently.

Losses and voltage drop over the DC transmission line depend only on the resistance of the cable. At given cable parameters, voltage drops over the cable according to simulation results are approx.  $0.04U_{dc\_rtd}$ .

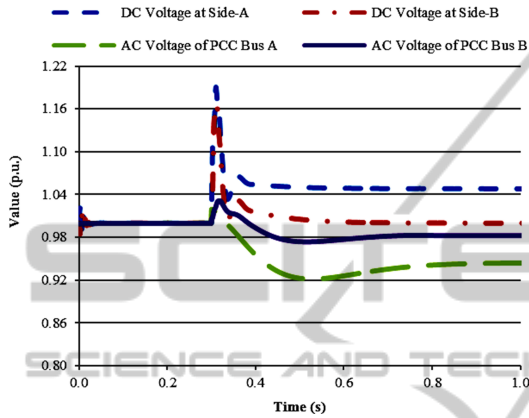


Figure 13: DC and AC Voltage Response Interconnecting Two Active Grid.

$PQ$  diagram provides information about the range and limits of operating point of the system for stable operation. Fig. 12. shows the  $PQ$  characteristic of 'Side-B' converter, connected to the capacitor bank of  $0.15P_n$  capacity.

Voltage strength of the network also depends on the short circuit capacity of the grid. A high short circuit capacity means, network is strong and stiff i.e. switching on/off a load, or shunt capacitors/reactors will not affect the voltage magnitude, significantly.

The effect of grid strength is directly reflected by the grid frequency. Strength of the network is defined by a short circuit ratio (SCR) i.e. it is the ratio of grid short circuit power to the converter rated power (Egea-

Table 1: Strength of Network.

Network Strength	SCR
High	$> 5$
Moderate	$3 - 5$
Low	$2 - 3$
Very Low	$< 2$

Alvarez et al., 2012).

$$SCR = \frac{S_{k\_grid}''}{P_{r\_con}} \quad (15)$$

The comparison of VSC-HVDC system ability to maintain the system frequency at nominal value with both strong and weak network connection can be visualized from Fig. 14 and Fig. 15. At lower SCR, change in grid frequency during transition period is approx.  $0.7Hz$ , which lead grid frequency drop to  $49.3Hz$  at 'Side-A' and rise to  $50.7Hz$  at 'Side-B'. In addition, weak grid has high internal impedance as compare to strong grid, thus it cause the higher voltage drop at PCC bus. Therefore, in order to stabilize the bus voltage 20% of  $P_n$  at 'Side-A' and 5% of  $P_n$  at 'Side-B' capacitive reactive power injection is required.

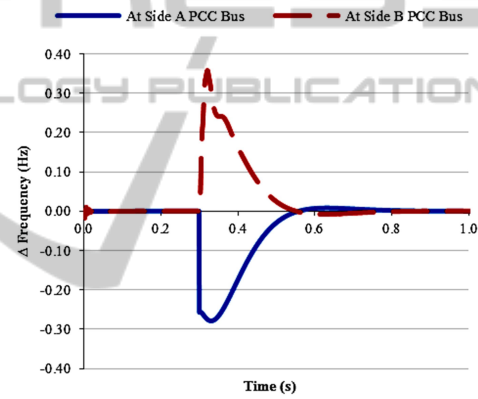


Figure 14: Effect of change in grid frequency at both sides PCC bus on changing load demand at SCR ratio of 5.0.

## 4.2 Interconnection of Passive Network

In this case study, analysis is made to evaluate the performance of developed control system for black start and to supply energy to passive network. For simulation, network configuration is same as shown in Fig. 1. Here, converter at load side 'Side-A' is set into passive mode and grid side converter 'Side-B' is set into  $U_{dc} - U_{ac}$  mode.

Load side converter act as an active source to the load. The passive control system tries to maintain the PCC bus voltage at  $1.0p.u.$ , and voltage magnitude and phase angle at the converter bus adopt itself, accordingly. The response of basic operation of consumer connected to the grid through HVDC system is shown in Fig. 16. Consumer load of  $0.7p.u$  active power and  $0.1p.u$  inductive reactive power is set for simulation purpose.

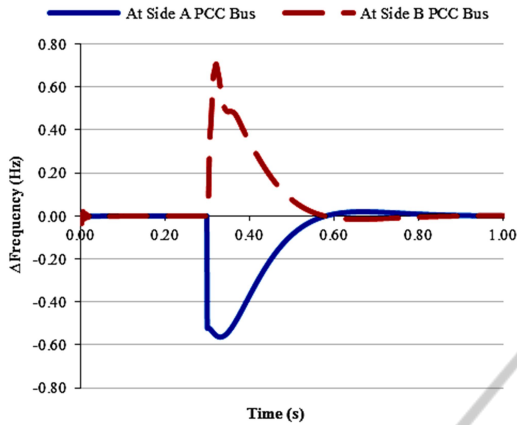


Figure 15: Grid frequency variation at both sides PCC bus at 2.5 SCR.

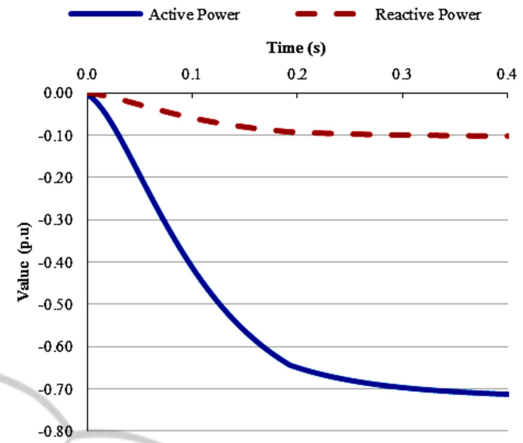


Figure 16: Active and reactive power at PCC bus of 'Side-A' connected with passive load.

AC signal generated by VSC is dependent on DC voltage. Sufficient DC voltage is required to generate the desired AC magnitude and phase angle to fulfill the demand. Converter model generates 1.0p.u AC magnitude at 1.0p.u DC voltage level at modulation index ( $P_m = 1$ ). At the given parameter, voltage drop across the transmission line is 5% of  $U_{dc}$ . In order to deliver the rated power, it is required to compensate the voltage drop and the power losses into the transmission system. This is done by adjusting the set point for DC voltage control at the grid side converter to higher level. Fig. 17. shows the voltage response at passive load PCC bus.

In Table. 2, capability of VSC-HVDC system to operate at different power factor is shown. As explained previously, that the passive network control system tries to maintain the PCC bus voltage at the load side to 1.0p.u. The effect of capacitive and inductive load can be seen from converter bus voltage.

It is to be seen that at  $u_{pcc}$ , nominal voltage re-

mains 1.0p.u at all power factor and converter control system adapt its voltage to generate or consume reactive power. Now, if we observe the simulation results at 0.9 capacitive power factor, converter bus voltages ( $u_{pwm}$ ) reduce to 0.87p.u. And, at 0.9 inductive power factor,  $u_{pwm}$  increases to 1.2p.u. Moreover, DC voltage across the capacitor at 'Side-B' is rise to its maximum permissible voltage. Theoretically, voltage collapse phenomena occur, when bus voltage does not remain within the following limits;

$$0.8 \leq u_n \leq 1.2$$

Since, internal bus voltages are within the above design criteria. Thus, it can be concluded that the system is stable for 0.9 leading to 0.9 lagging power factor.

Table 2: Simulation Results of 'Side-A' System at Different Capacitive and Inductive Power Factors.

	Power Factor	Passive Load				DC Voltage Across Capacitors	
		$u_{pcc}$	$u_{pwm}$	Active Power	Reactive Power	Side-A	Side-B
Capacitive	0.90	1.00	0.87	1.00	0.48	1.00	1.05
	0.925	1.00	0.89	1.00	0.41	1.00	1.05
	0.95	1.00	0.93	1.00	0.33	1.00	1.05
	0.98	1.00	0.97	1.00	0.20	1.00	1.05
	1.00	1.00	1.05	1.00	0.00	1.05	1.10
Inductive	0.98	1.00	1.12	1.00	0.20	1.07	1.12
	0.95	1.00	1.17	1.00	0.33	1.11	1.16
	0.925	1.00	1.19	1.00	0.41	1.14	1.18
	0.90	1.00	1.20	1.00	0.48	1.15	1.20

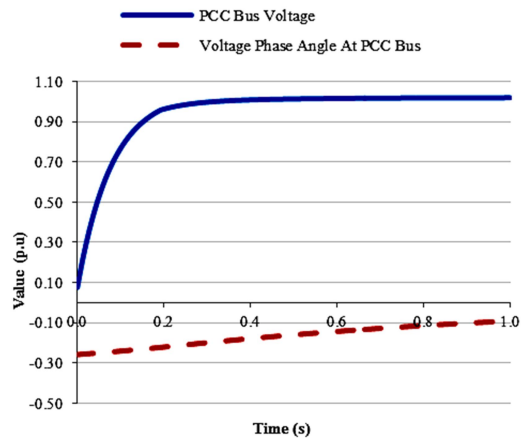


Figure 17: Response of AC voltage and voltage phase angle at PCC bus connect to passive load

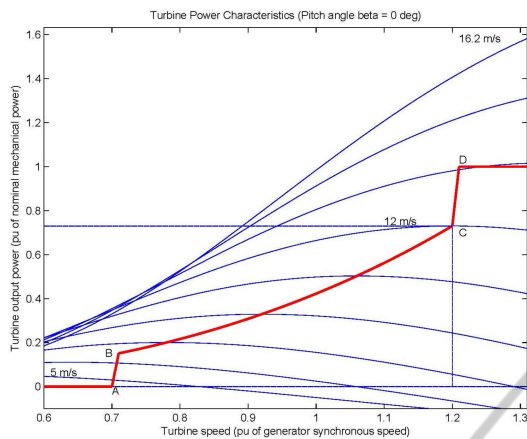


Figure 18: Doubly-Fed-Induction generator torque speed characteristic

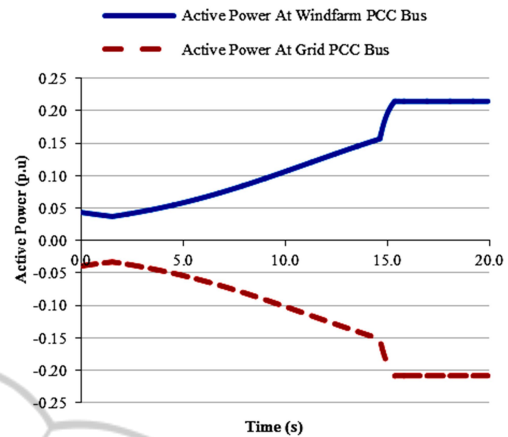


Figure 20: Wind farm active power generation and in-feed into the grid

### 4.3 Interconnection of Wind Farm

In this case study, system response connecting wind farm with the grid over long distance is analysed. MATLAB standard DFIG model is used for simulation purpose. The behavior of wind turbine output power with respect to turbine speed and wind velocity is shown in Fig. 18. At 'Side-A' in Fig. 1, an equivalent model of wind farm array is connected with the overall capacity is 45MWatt. To simulate the model, converter connected with wind farm is set into passive control mode and grid side converter is set into the  $U_{dc} - U_{ac}$  control mode.

The response of wind farm power in-feed into the grid via HVDC transmission system can be observe from Fig. 20. It can be notice that power generation increases due to change in wind speed from 3m/s to 14m/s. As a result, active power received from wind

farm is transferred to grid with minimum losses, and HVDC system provides the stable operation. Fig. 19 demonstrate the ability of VSC-HVDC system to fulfil the DFIG reactive power demand and control system is able to maintain the voltage level within the design limits.

Despite the higher investment cost of HVDC transmission system as compare to AC transmission system for interfacing wind turbines with the grid(Bresesti et al., 2007), HVDC system provide benefit of reducing the impact of varying wind generation and gives ability to control the reactive power, consequently, supports the grid voltage.

## 5 CONCLUSION AND RECOMMENDATION

The aim of the work resulting in this research is to develop the VSC-HVDC control system and study the feasibility of using it as an alternative of conventional HVAC system. 'Case-A' study concluded that with independent control of the active and reactive power, it is possible to transfer large power between strong and weak grid and achieved improve voltage and frequency stability. Results have shown that the reactive power generation capability of VSC-HVDC system increases by increasing capacitor bank capacity and, ability to operate at full active power at maximum over-excited condition is increased by decreasing the transmission length. The design system is capable of operating at 0.9 under and over excited power factors. The simulation results of 'Case-B' show that the change in power factor at load side does not affect the voltage stability at grid side system. Also,

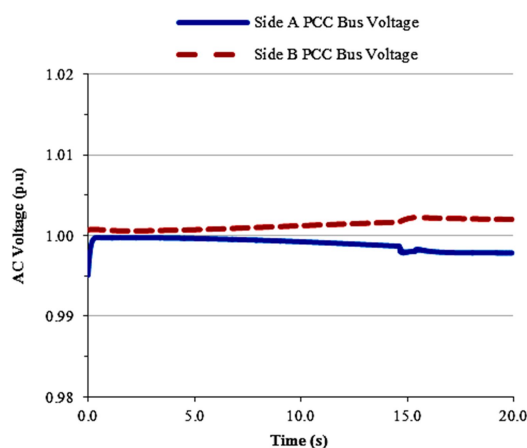


Figure 19: Dynamic AC voltage response due to wind energy injection into the grid

leading and lagging reactive power generation capability of converter can be improved by incorporating transformer tap control into converter control system. Results from 'Case-C' study conclude that the developed control system is capable of integrating wind farm with the grid over long distance and fulfil reactive power demand of wind turbine without addition compensation.

In addition, VSC-HVDC system is model for simulation of small signal disturbance. The developed control system can be extended for critical case investigation such as fault-ride-through capability and multi-terminal HVDC system. This research outcome is useful for pre-designing electrical power system, power system modelling and simulation and to study the impact of wind energy on system dynamics.

## REFERENCES

- Bao, J., Gao, Z., and Meng, C. (2011). Application of vsc-hvdc system on offshore wind farm. Power Engineering and Automation Conference (PEAM).
- Bresesti, P., Kling, W., Hendriks, R. L., and Vailati, R. (2007). Hvdc connection of offshore wind farms to the transmission system. *IEEE Transactions on Energy Conversion*, 22.
- Egea-Alvarez, A., Bianchi, F. A., and Gomis-Bellmunt, O. (2012). Experimental implementation of a voltage control for a multi-terminal vsc-hvdc offshore transmission system. 3rd IEEE PES International Conference and Exhibition on Innovative Smart Grid Technologies (ISGT Europe).
- E.ON (2006). Grid code: High and extra high voltage. Technical report, E.ON Netz GmbH, Bayreuth.
- E.ON (2008). Requirement for offshore grid connections in the e.on netz network. Technical report, E.ON Netz GmbH, Bayreuth.
- Hulle, F. and Gardner, P. (2010). Wind energy the facts, grid integration. Technical report, EWEA.
- Wang, S., Li, X., Chen, X., and Tang, G. (2009). Reduced-order model of hvdc light system based on multi-time scale. 4th IEEE Conference on Industrial Electronics and Applications (ICIEA).
- Wilkes, J. (2010). Wind in power: 2009 european statistics. Technical report, EWEA.
- Yuan, Z. and Wang, H. (2012). The research on the vsc-hvdc control system structure. Asia Pacific Power and Energy Engineering Conference (APPEEC).
- Zhang, L. and Lennart, H. (2011). Modelling and control of vsc-hvdc links connected to island systems. *IEEE Transactions on Power Systems*, 26.